Formation of $[M - nH + mNa]^{(m-n)+}$ and $[M - nH + mK]^{(m-n)+}$ Ions in Electrospray Mass Spectrometry of Peptides and Proteins

Christopher F. Rodriquez, Xu Guo, Tamer Shoeib, Alan C. Hopkinson and K. W. Michael Siu

Department of Chemistry and Centre for Research in Mass Spectrometry, York University, Toronto, Ontario, Canada

The $[M - nH + mNa]^{(m-n)+}$ and $[M - nH + mK]^{(m-n)+}$ ions are common in the electrospray mass spectra of proteins and peptides. The feasibility of forming these ions in the gas phase via collision activation and/or ion–molecule reaction is investigated. Sodium and potassium affinities of the N-methylacetamide anion, the acetate anion, and the 1-propanamide anion have been calculated using density functional theory at the B3LYP/6-311++G(d,p) level of theory. These anions were chosen as models for the functional groups on a protein or peptide. These affinity values are then used to calculate reaction enthalpies of alkali hydroxides, chlorides, and hydrates with N-methylacetamide, acetic acid, the acetate anion, and 1-propanamine, model reactions that may lead to formation of the $[M - nH + mNa]^{(m-n)+}$ and $[M - nH + mK]^{(m-n)+}$ ions. It is found that a number of these reactions are exothermic or slightly endothermic ($\Delta H^\circ < +20$ kcal/mol) and are accessible after collision activation in the lens region. The potential energy hypersurfaces of model reactions between NaOH and formamide as well as NaCl and formamide show relatively flat surfaces devoid of significant barriers. (J Am Soc Mass Spectrom 2000, 11, 967–975) © 2000 American Society for Mass Spectrometry

Since its inception, electrospray mass spectrometry has revolutionized the analysis of peptides and proteins [1, 2]. The most common analysis involves electrospraying a dilute acidic protein solution and characterizing the resulting protonated protein ions [3]. Adduction with other cations, especially alkali metal ions, is also frequently observed particularly when alkali metal salts are present as impurities or additives. The complex ions observed often have alkali metal ions not only present as simple adducts, but also as replacement for protons that have been abstracted [4, 5]. Transition metal ions, such as Cu^{2+} and Ni^{2+}, are known to induce abstraction of an amide proton from an oligopeptide in solution, after ligation to the N-terminal nitrogen atom; the analogous reactions, however, are unknown for alkali metal ions [6].

In a recent report, we proposed that complex ions of the type $[M - nH + mX]^{(m-n)+}$ can be formed in the lens region of a mass spectrometer from electrosprayed alkali metal ion–peptide adducts after their collisional activation, as well as from collisions between peptide ions and neutral alkali metal compounds [5]. Using lithium hydroxide, chloride, and hydrate as examples, we calculated reaction enthalpies for their reactions with N-methylacetamide, acetic acid, the acetate anion, and 1-propanamine (all models of functional groups on a peptide) and showed that the majority of these reactions are either exothermic or slightly endothermic. Furthermore, we also showed, using a model reaction between formamide and lithium hydroxide, that the reactions are dominated by a relatively deep well from the formation of a binary complex and are essentially devoid of barriers. As a result, the reaction rates are essentially determined by reaction enthalpies. We estimated that, under typical electrospray sampling conditions in the lens region, reactions with endothermicities smaller than 20 kcal/mol are accessible, and peptide–lithium salt reactions that are exothermic or endothermic by less than this value should proceed readily to yield $[M - nH + mLi]^{(m-n)+}$ ions.

As described in [5], the decision then to examine lithiated adducts was made based on computational economy. In this current study, we are extending this earlier work to the formation of $[M - nH + mNa]^{(m-n)+}$ and $[M - nH + mK]^{(m-n)+}$ ions that are observed much more frequently than $[M - nH + mLi]^{(m-n)+}$ due to the much more extensive use of sodium- and potassium-containing reagents and wider occurrence of Na^+ and K^+ in nature.

Address reprint requests to K. W. Michael Siu, Department of Chemistry, York University, 4700 Keele St., Toronto, Ontario M3J 1P3, Canada. E-mail: kwmsiu@yorku.ca

1044-0305/00/$20.00
PII S1044-0305(00)00162-8

Received January 6, 2000
Revised May 16, 2000
Accepted May 16, 2000

Experimental

Experiments were conducted on a PE-SCIEX API 3000 prototype triple quadrupole mass spectrometer (Concord, Ontario). Ubiquitin was commercially available from Sigma (St. Louis, MO). Samples were 10 μM of ubiquitin plus 1 mM of sodium hydroxide, sodium chloride, potassium hydroxide, or potassium chloride in 50/50 methanol and water. These were continuously infused at a rate of 2 μL/min into the pneumatically assisted electrospray probe with air being the nebulizer gas. Mass spectra were acquired at the range 600–3000 m/z units, at a step size of 0.2 unit, and a dwell time of 10 ms; 10 scans were summed to produce a mass spectrum.

Computational Methods

Density functional theory (DFT) employing the hybrid B3LYP method, which uses Becke's three-parameter exchange functional [7] and the correlation functional of Lee et al. [8], with the 6-311++G(d,p) basis set [9] in Gaussian 98 [10], was used to calculate the optimized geometries and vibrational frequencies. First-order saddle points were found using the Berny transition-state algorithm and the CALCALL method [10].

Results and Discussion

Figure 1 shows the electrospray mass spectra of ubiquitin with (a) potassium chloride and (b) potassium hydroxide. Both spectra contain a large number of clusters bearing $[M - nH + mK]^{(m-n)+}$ ions; the extent of potassium incorporation in ubiquitin, however, is much higher in the presence of potassium hydroxide than potassium chloride. This is evident in the two insets, which show the 5+ clusters in detail. For these clusters $(m - n) = 5$; in other words, the ions have a general formula of $[M - (m - 5)H + mK]^{5+}$. Ubiquitin is a small, 76-residue protein that has an average molecular mass of 8564.9 Da. The number of incorporated potassium atoms, m, in a given ion can be solved by

$$m = (5 \times (m/z) - 5 - 8564.9)/(39.1 - 1.0) \quad (1)$$

with (m/z) being the mass-to-charge ratio of the ion. Thus, in the inset of Figure 1a, the first peak at $(m/z) = 1713.8$ has an m of $(5 \times 1713.8 - 5 - 8564.9)/(39.1 - 1.0) = 0.0$. For the 15th peak, $(m/z) = 1820.2$, $m = (5 \times 1820.2 - 5 - 8564.9)/(39.1 - 1.0) = 13.9$. The number of incorporated potassium atoms for each cluster ion, rounded to the nearest integer, is shown. The envelope of cluster ions observed in the presence of potassium chloride is comparatively wider than that in the presence of potassium hydroxide; the relative extent of potassium incorporation, as judged from that of the most abundant ions, however, is smaller in the former than in the latter. In Figure 1a, m ranges from 0 to more than 20 with $m = 5$ being the most abundant, whereas in Figure 1b, m ranges from 9 to at least 21 with $m = 14$ being the most abundant.

Incorporation of potassium in clusters of higher charges is equally extensive in Figure 1b. For the +6 cluster, $m = 15$ for the ions at $(m/z) = 1523.6$; for the +7 cluster, $m = 16$ for $(m/z) = 1311.6$; and for the +8 cluster, $m = 17$ for $(m/z) = 1152.6$. This is to be contrasted with the situation in Figure 1a, where the extent of potassium incorporation apparently drops off with increasing cluster charge. We will show in later sections that the lower degree of potassium incorporation in the presence of potassium chloride, relative to that with potassium hydroxide, is in accordance with the differences in reaction enthalpies of these salts with model functional groups on ubiquitin. Calculations show that potassium hydroxide is able to react with more kinds of functional groups than potassium chloride and that the energetics are more favorable for the former reaction. It should be pointed out that the mass spectra of ubiquitin in the presence of sodium chloride and sodium hydroxide (not shown) bear strong resemblances to those of potassium chloride and potassium hydroxide. The multiply charged potassium-containing adducts, however, are better resolved from one another as potassium has a higher mass than sodium.

As before, we began our assessment of the feasibility of creating $[M - nH + mK]^{(m-n)+}$ and $[M - nH + mNa]^{(m-n)+}$ ions in the gas phase by examining reaction enthalpies of KOH, KCl, $K(H_2O)^+$, NaOH, NaCl, and $Na(H_2O)^+$ with compounds that mimic functional groups on a peptide. The compounds are: N-methylacetamide, which models the peptide linkage; acetic acid and the acetate anion, which model the carboxylic terminus as well as the side-chain functional groups on acidic residues; and 1-propanamide, the amino terminus and the side-chain functional groups on basic residues [5]. The 12 reactions that are considered for each alkali metal, using K as an example, are

$$CH_3CONHCH_3 + KOH \rightarrow CH_3CON(K)CH_3 + H_2O \quad (2)$$

$$CH_3CONHCH_3 + KCl \rightarrow CH_3CON(K)CH_3 + HCl \quad (3)$$

$$CH_3CONHCH_3 + K(H_2O)^+ \rightarrow CH_3CON(K)CH_3 + H_3O^+ \quad (4)$$

$$CH_3COOH + KOH \rightarrow CH_3COOK + H_2O \quad (5)$$

$$CH_3COOH + KCl \rightarrow CH_3COOK + HCl \quad (6)$$

$$CH_3COOH + K(H_2O)^+ \rightarrow CH_3COOK + H_3O^+ \quad (7)$$

$$CH_3COO^- + KOH \rightarrow CH_3COOK + OH^- \quad (8)$$

$$CH_3COO^- + KCl \rightarrow CH_3COOK + Cl^- \quad (9)$$

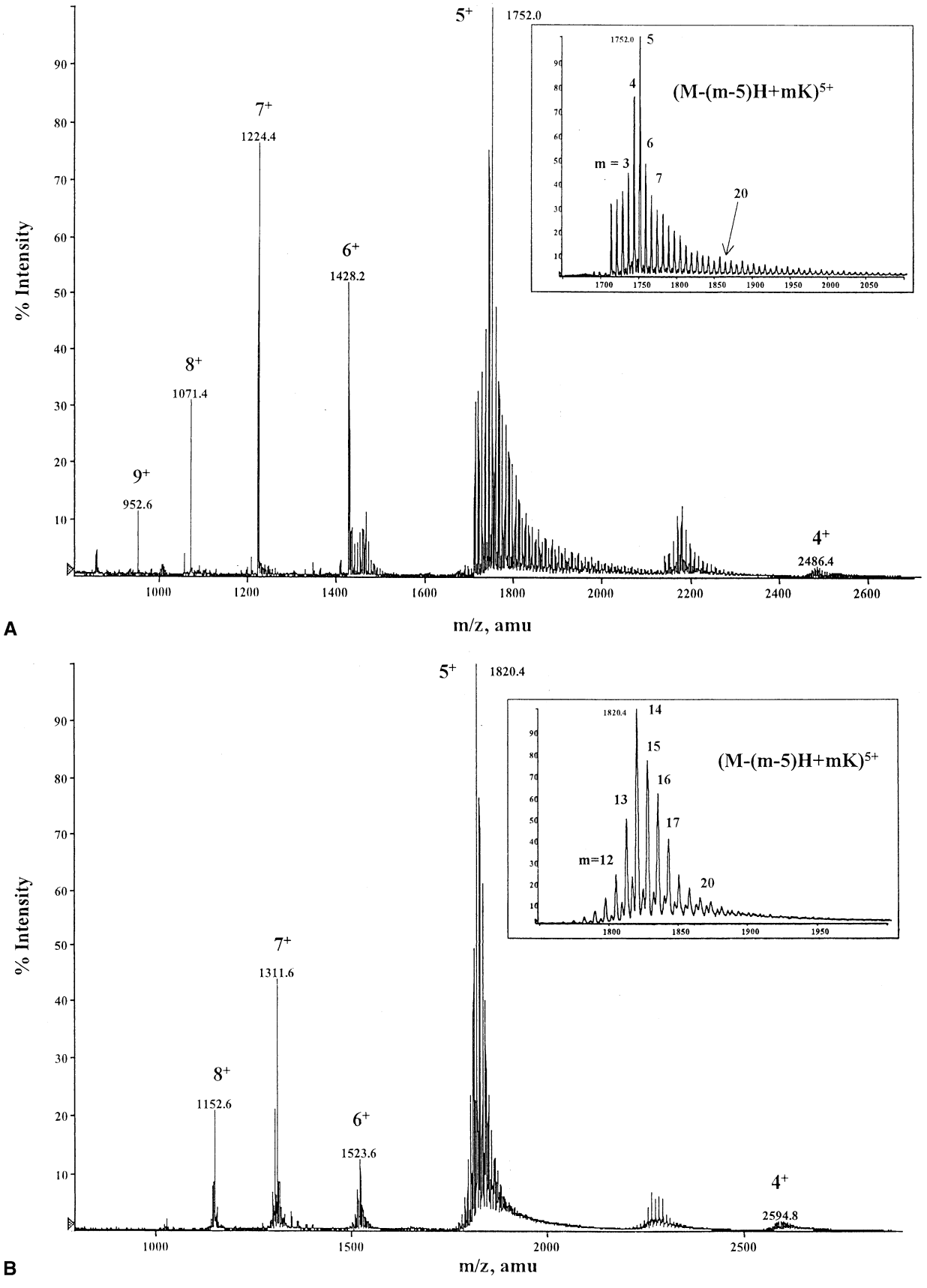

Figure 1. Electrospray mass spectra of ubiquitin with (**a**) potassium chloride and (**b**) potassium hydroxide. Insets show the $[M - (m - 5)H + mK]^{5+}$ clusters with different m values.

$$CH_3COO^- + K(H_2O)^+ \rightarrow CH_3COOK + H_2O \quad (10)$$

$$CH_3CH_2CH_2NH_2 + KOH \rightarrow CH_3CH_2CH_2NHK + H_2O \quad (11)$$

$$CH_3CH_2CH_2NH_2 + KCl \rightarrow CH_3CH_2CH_2NHK + HCl \quad (12)$$

$$CH_3CH_2CH_2NH_2 + K(H_2O)^+ \rightarrow CH_3CH_2CH_2NHK + H_3O^+ \quad (13)$$

The reaction enthalpies are calculable from standard thermochemical data, provided that the potassium ion affinities (KAs) of the N-methylacetamide anion, **1**, the acetate anion, **2**, and the 1-propanamide anion, **3**, are independently known. For example,

$$\Delta H^\circ_2 = \Delta H^\circ_{acid}\,(\text{N-methylacetamide}) + \text{KA}\,(OH^-) - \Delta H^\circ_{acid}\,(H_2O) - \text{KA}\,(\mathbf{1}) \quad (14)$$

$$\Delta H^\circ_9 = \Delta H^\circ_{acid}\,(\text{acetic acid}) + \text{KA}\,(Cl^-) - \Delta H^\circ_{acid}\,(HCl) - \text{KA}\,(\mathbf{2}) \quad (15)$$

$$\Delta H^\circ_{13} = \Delta H^\circ_{acid}\,(\text{1-propanamine}) + \text{KA}\,(H_2O) - \text{PA}\,(H_2O) - \text{KA}\,(\mathbf{3}) \quad (16)$$

where PA is proton affinity [5]. To obtain the reaction enthalpies, we calculated in this study the KAs and sodium ion affinities (SAs) of **1**, **2**, and **3**, and those of OH^-, Cl^-, and H_2O, using molecular orbital calculations. The latter simple species were included such that their affinities may serve as comparisons with reference experimental data to allow us to gauge the accuracy of the DFT method at the B3LYP/6-311++G(d,p) level of theory. Table 1 shows the electronic energies, zero-point vibrational energies, and thermal corrections (necessary to adjust the reactions to 298 K) of **4**, **5**, and **6**, the potassium salts of respectively **1**, **2**, and **3**; those of **7**, **8**, and **9**, the sodium salts of **1**, **2**, and **3**; and those of alkali hydroxides, chlorides, and hydrates. The structures of the anions and the salts are shown in Figure 2, together with those of **10**, **11**, and **12**, the lithium salts of **1**, **2**, and **3**, which are reproduced here for comparison [5].

Attachment of Na and K to the N-methylacetamide anion, **1**, effects a conformational change to **1** that is essentially the same as that resulting from the attachment of Li, in which the two methyl groups become *cis* to each other. One minor difference is that in **10**, the C-methyl group is staggered about the O–Li bond, whereas in the Na- and K-containing analogs **4** and **7**, the C-methyl group eclipses the O-metal bond. Replacement of Li with Na, and with K, leads to lengthening of the X–O (where X = the alkali metal) and the X–N bonds, and widening of the X–O–C, O–C–N, and C–N–X bond angles; otherwise the resulting salt structures, **10**, **7**, and **4**, are nearly identical. The increases in metal–ligand bond lengths and metal–related bond angles are in accordance with the increase in atomic radii from Li to Na and K. Parallel effects are also apparent in the salts of the acetate anion, **2**, and the 1-propanamide anion, **3**.

Table 1. Electronic energies[a], zero-point vibrational energies[b] (ZPVE), and thermal energies[b,c] for (A) potassium- and (B) sodium-containing species

Species	Electronic	ZPVE	Thermal
(A)			
4	−847.97698	56.0	4.9
5	−828.56759	31.2	4.0
6	−773.86718	67.0	4.7
K^+	−599.76106		0.9
KOH	−675.81491	6.7	2.2
KCl	−1060.24770	0.4	1.8
$K(H_2O)^+$	−676.24944	14.8	2.5
(B)			
7	−410.33532	56.3	4.8
8	−390.92341	31.6	3.7
9	−336.22378	67.4	4.6
Na^+	−162.08757		0.9
NaOH	−238.16799	6.8	2.2
NaCl	−622.60101	0.5	1.7
$Na(H_2O)^+$	−162.08757	15.0	2.4

[a]Electronic energies in Hartrees.
[b]ZPVE and thermal energies are in kcal mol^{-1}.
[c]Sum of translational, vibrational, and rotational energies at 298 K.

The calculated SAs and KAs are shown in Table 2 along with corresponding LAs [5] and relevant experimental values calculated from reference thermochemical data [11–14]. Judging from the degree of agreement between calculated LAs, SAs, and KAs and experimental affinities for OH^-, Cl^-, and H_2O (average absolute deviation = 1.5 kcal/mol), the DFT B3LYP/6-311++G(d,p) method should provide adequate accuracies for the crucial SAs and KAs of the N-methylacetamide, the acetate, and the 1-propanamide anions for this study. (Basis set superposition errors, as judged by the value of 1.5 kcal/mol calculated for potassium propanamide, **6**, are negligible.) For a given ligand, it is apparent that the calculated ion affinity decreases from Li to Na to K; this is in accordance with the ability of the metal to hold a positive charge.

Table 3 shows the reaction enthalpies of XOH, XCl, and $X(H_2O)^+$, where X = Li, Na, and K, with N-methylacetamide, acetic acid, the acetate anion, and 1-propanamine; the lithium-related data are reproduced here from the earlier work [5] for comparison. Reaction enthalpies that are either negative or positive by less than 20 kcal/mol are shown in bold. We estimate that reactions which are exothermic by less than 20 kcal/mol may be rendered sufficiently fast to be observable because of multiple collision activation in the lens region, provided that the barriers of such reactions are not significant [5]. The selection of 20 kcal/mol as the limit is somewhat arbitrary, but justifiable in view of the following observations. In a recent

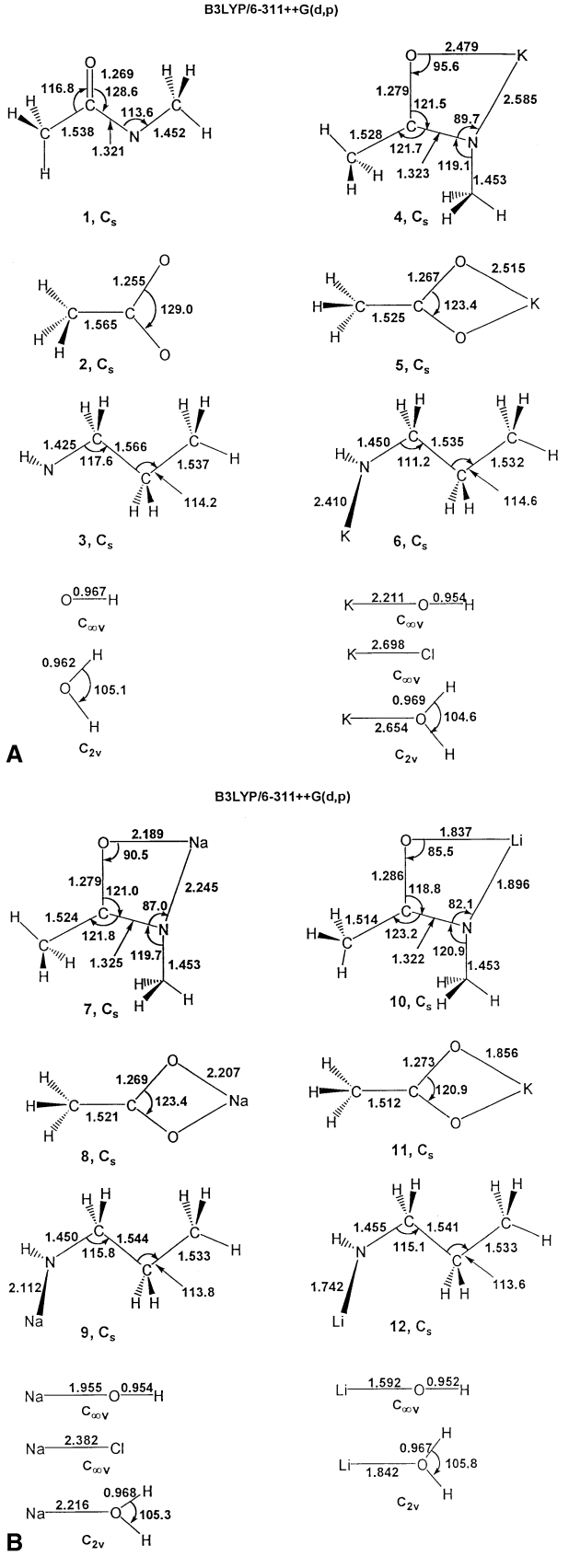

Figure 2. Geometric parameters for anions, lithium, sodium and potassium salts, water, and hydrates. Bond distances are in angstroms and angles in degrees.

Table 2. Calculated Li, Na, and K ion affinities of anions (kcal/mol) using DFT at the B3LYP/6-311++G(d,p) level of theory. Experimental values (Expt.) are also shown for comparison

Anion	Li[a]	Expt.	Na	Expt.	K	Expt
1	170.4		143.8		124.0	
2	170.5		145.3		127.0	
3	175.6		147.3		128.7	
OH^-	187.9	185.7[a]	158.0	158.7[b]	141.5	144.7[e]
Cl^-			131.8	132.7[c]	119.8	118.3[f]
H_2O	35.5	33.9[a]	25.0	24.1[d]	18.0	17.2[g]

[a]Reference [5].
[b]$\Delta_f H°$ (Na^+) + $\Delta_f H°$ (OH^-) − $\Delta_f H°$ (NaOH) = 144.1 − 32.7 + 47.3 = 158.7.
[c]$\Delta_f H°$ (Na^+) + $\Delta_f H°$ (Cl^-) − $\Delta_f H°$ (NaCl) = 144.1 − 54.4 + 43.0 = 132.7.
[d]$\Delta_f H°$ (Na^+) + $\Delta_f H°$ (H_2O) − $\Delta_f H°$ $(NaOH_2^+)$ = 144.1 − 57.8 − 62.2 = 24.1.
$\Delta_f H°$ $(NaOH_2^+)$ = $\Delta_f H°$ (H^+) + $\Delta_f H°$ (NaOH) − PA (NaOH) = 365.7 − 47.3 − 256.2 = 62.2.
[e]$\Delta_f H°$ (K^+) + $\Delta_f H°$ (OH^-) − $\Delta_f H°$ (KOH) = 121.4 − 32.7 + 56.0 = 144.7.
[f]$\Delta_f H°$ (K^+) + $\Delta_f H°$ (Cl^-) − $\Delta_f H°$ (KCl) = 121.4 − 54.4 + 51.3 = 118.3.
[g]$\Delta_f H°$ (K^+) + $\Delta_f H°$ (H_2O) − $\Delta_f H°$ (KOH_2^+) = 121.4 − 57.8 − 46.4 = 17.2.
$\Delta_f H°$ (KOH_2^+) = $\Delta_f H°$ (H^+) + $\Delta_f H°$ (KOH) − PA (KOH) = 365.7 − 56.0 − 263.3 = 46.4.
All reference thermochemical data from [11–14].

study involving $Ag(NH_3)_n^+$ complex ions, very few $Ag(NH_3)_3^+$ ions and no $Ag(NH_3)_4^+$ ions were observed, even under very mild sampling conditions, when a solution of $AgNO_3$ was electrosprayed in the presence of 5% ammonia [15]. Under regular lens conditions, such as those used here, virtually no $Ag(NH_3)_3^+$ ions were observed. The abundances for $Ag(NH_3)_2^+$ and $Ag(NH_3)^+$ were always very high. DFT calculations at

Table 3. Reaction enthalpies (kcal/mol) of XOH, XCl, and $X(H_2O)^+$, where X = (A) Li, (B) Na, and (C) K, with N-methylacetamide, acetic acid, the acetate anion, and 1-propanamine[a]

Species	Functional group	XOH	XCl	$X(H_2O)^+$
(A) Lithium				
N-methylacetamide	Peptide bond	**−12.2**	**14.1**	61.7
Acetic acid	Acid	**−26.2**	**0.1**	47.7
Acetate anion	Acid	**15.9**	**−14.8**	**−135.9**
1-Propanamine	Amine	**18.5**	44.8	92.4
(B) Sodium				
N-methylacetamide	Peptide bond	**−12.4**	**19.0**	78.9
Acetic acid	Acid	**−27.2**	**4.2**	63.9
Acetate anion	Acid	**14.9**	**−10.7**	**−119.7**
1-Propanamine	Amine	20.6	52.0	111.7
(C) Potassium				
N-methylacetamide	Peptide bond	**−7.0**	24.0	91.2
Acetic acid	Acid	**−23.3**	**7.7**	74.9
Acetate anion	Acid	**18.8**	**−7.2**	**−108.7**
1-Propanamine	Amine	24.8	55.8	123.0

[a]Values that are exothermic and endothermic by less than 20 kcal/mol are shown in bold.

the B3LYP/DZVP level of theory show that the reaction enthalpies, $\Delta H^{\circ}_{n,n+1}$, for the reaction

$$Ag(NH_3)_n^+ + NH_3 \rightarrow Ag(NH_3)_{n+1}^+ \quad (17)$$

are $\Delta H^{\circ}_{0,1} = -40.1$; $\Delta H^{\circ}_{1,2} = -36.1$; $\Delta H^{\circ}_{2,3} = -15.1$; and $\Delta H^{\circ}_{3,4} = -11.0$ kcal/mol; the last three values are in excellent agreement with experimental reaction enthalpies [16]. The absence of observed $Ag(NH_3)_3^+$ and $Ag(NH_3)_4^+$ ions was attributed to collision-induced fragmentation in the lens region, thus implying that an energy between 15 and 36 kcal/mol is available via collisional activation. Furthermore, complexes such as $Ag(H_2O)^+$ and $Na(CH_3OH)^+$, for which bond enthalpies are 28.4 [17] and 22.3 kcal/mol [18], respectively, give intense signals. For the latter complex, the abundance ratio of $Na(CH_3OH)^+$ and Na^+ is typically 1.2–1.5. These observations all support the estimate that the magnitude of collisional activation in the lens region is approximately 20 kcal/mol.

It is apparent in Table 3 that the number of functional groups whose reactions with the alkali metal-containing reagents are either exothermic or endothermic by less than 20 kcal/mol decreases from the reagent being alkali hydroxide to alkali chloride to alkali hydrate. It is noteworthy that the most abundant functional group on a peptide is the amide linkage, and that the reactions of N-methylacetamide with all three alkali hydroxides are exothermic, whereas those with all three alkali chlorides are endothermic albeit accessible for LiCl and probably for NaCl. The experimentally observed lower extent of alkali metal incorporation from the chloride salt, e.g., in Figure 1a for potassium incorporation to ubiquitin, is in accordance with the aforementioned trends in Table 3.

In the earlier study, the potential energy hypersurface of the LiOH + $HCONH_2$ reaction was used as a prototypical example for the formation of $[M - nH + mLi]^{(m-n)+}$ [5]. In that reaction, the reaction profile is dominated by a relatively deep well of approximately 35 kcal/mol, due to the formation of a formamide–lithium hydroxide complex with initial lithiation occurring on the carbonyl oxygen; subsequent hydrogen transfer from the amide group to the oxygen atom of LiOH, di-coordination of the Li by both the amide oxygen and nitrogen atoms, and finally elongation of the Li–OH_2 bond to yield HCON(Li)H and H_2O complete the reaction profile [5]. The important feature is that none of the reaction steps exhibit large barriers and the reaction is driven entirely by its exothermicity. Thus it was deemed probable that the assumption of small barriers for lithium salt reactions with peptide functional groups is correct. Here we furnish two other examples to establish that this assumption is indeed generally applicable. Figure 3 shows the energy hypersurfaces for the following two reactions:

$$\text{(a) } HCONH_2 + NaOH \rightarrow HCON(Na)H + H_2O \quad (18)$$

$$\text{(b) } HCONH_2 + NaCl \rightarrow HCON(Na)H + HCl \quad (19)$$

Figure 4 displays the structures while Table 4 lists their energetics. Similar to what was calculated previously in the reaction of $HCONH_2$ with LiOH [5], the first steps in the reaction profiles are the formation of the formamide–sodium hydroxide complex, **M1**, in reaction (18) (see Scheme **1**) and that of the formamide–sodium chloride complex, **M4**, in reaction (19). An amide hydrogen then migrates over to the electron-rich center, the hydroxide oxygen and the chloride, to form the transition state structures **TS2** and **TS4**, respectively (**TS2** is actually formed via **TS1** and **M2**). From **TS2** lengthening of the Na–O bond and rearrangement produce the final products **P1**. Similarly, from **TS4** cleavage of the Na–Cl bond and rearrangement leads to the final products **P2**. Comparing the two profile types, reaction (18) produces a much flatter profile than reaction (19); furthermore, the former reaction is exergonic ($\Delta G^{\circ}_{298} = -10.3$ kcal/mol), whereas the latter is endergonic ($\Delta G^{\circ}_{298} = 16.0$ kcal/mol).

For reaction (18) the lack of significant barriers and its exergonicity mean that it would be highly efficient. For reaction (19) **TS4** imposes a free-energy barrier of 35.3 kcal/mol relative to **M4**. A portion of this activation energy is recovered from the exergonicity of the complexation reaction to form **M4** ($\Delta G^{\circ}_{298} = -16.4$ kcal/mol) with the rest provided by collisional activation. The lower energy channel in the dissociation of **M4** is one which yields the reactants, formamide, and sodium chloride (**R2**), resulting in no net reaction; the second, higher energy channel is the rearrangement reaction to form the products sodium formamide and hydrogen chloride (**P2**). The fact that sodium and potassium incorporation are observed (e.g., Figure 1a) in the presence of alkali chloride is probably due to the large number of amide groups present and the large number of collisions. As discussed earlier, the relative free energy between the products and reactants are reversed in the reaction between formamide and sodium hydroxide (Figure 3b). There the lower energy channel in the dissociation of **M1** is the rearrangement reaction to form sodium formamide and water (**P1**), a result very similar to that between formamide and lithium hydroxide [5]. That incorporation of sodium is the lower reaction channel for sodium hydroxide, but not for sodium chloride, as reagent is consistent with the higher degree of observed sodium incorporation in the former than in the latter (for an example of potassium substitution, compare Figure 1a with 1b).

In electrospray, ions are believed to be desorbed into the gas phase clustered to a large number of solvent molecules [2, 3, 19–21]. These solvent molecules are subsequently removed in the lens region of the mass spectrometer via a number of collision-induced disso-

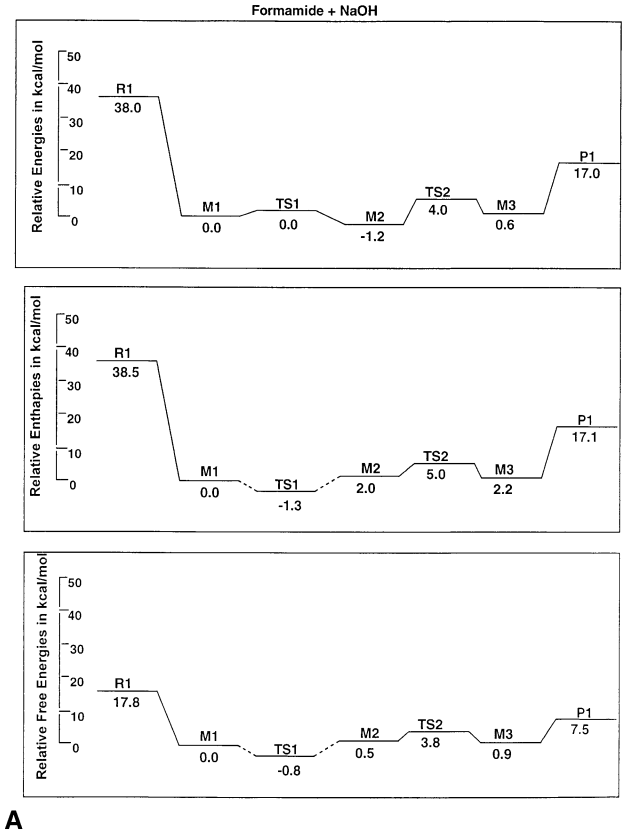

Figure 3. Hypersurfaces for the reactions (**a**) $HCONH_2$ + NaOH → HCON(Na)H + H_2O and (**b**) $HCONH_2$ + NaCl → HCON(Na)H + HCl. Values shown are relative energies, enthalpies, and free energies in kcal/mol; details are in Table 4.

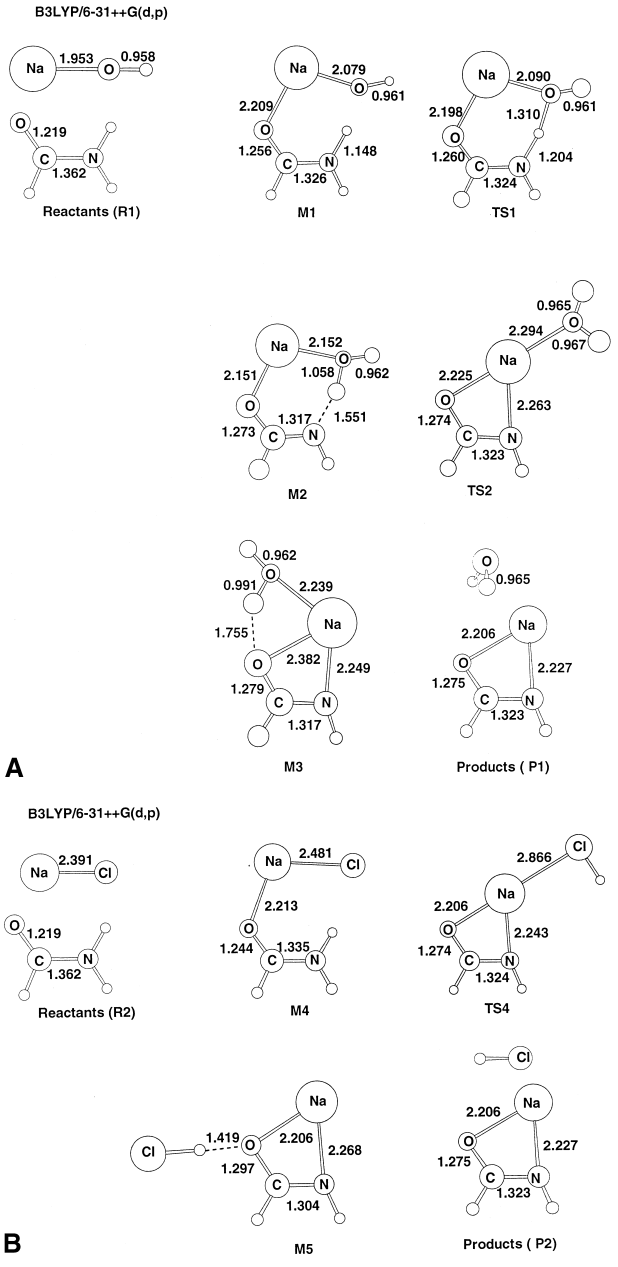

Figure 4. Structures of reactants, intermediates, transition states, and products in Figure 3.

ciations. Furthermore, there is also a possibility that solvent condensation on the ions (nucleation) can occur in the supersonic jet [20, 21]; these condensed solvent molecules are subsequently cleaved in collisions downstream. In cases where the sample solution contains nonvolatile additives, such as potassium hydroxide, we have shown that these are also sampled and are complexed to multimers of the ions; this was demonstrated in a collision-induced dissociation of a 30-*m/z*-wide window of background ions, which yielded $[M - nH + mK]^{(m-n)+}$ and $K(KOH)_p^+$ (p = 1–4) ions [5]. Two scenarios are possible that could eventually lead to formation of the $[M - nH + mX]^{(m-n)+}$ ions in the lens

Table 4. Total electronic energies (in hartrees), zero-point vibrational energies, and thermal corrections (both in kcal mol^{-1}), entropies (in cal mol^{-1} K^{-1}), and relative electronic energies (ΔE), enthalpies (ΔH°_{298}) and free energies (ΔG°_{298}) (all in kcal mol^{-1}) at B3LYP/6-31++G(d,p) for structures in Figure 3a, b

Structures	Electronic energies	Zero-point energies	Thermal corrections	Entropy	ΔE	ΔH°_{298}	ΔG°_{298}
R1	−408.04481	35.7	4.6	116.7	38.0	38.5	17.8
M1	−408.10538	36.1	4.3	80.7	0.0	0.0	0.0
M2	−408.10735	36.8	4.4	82.6	−1.2	2.0	0.5
M3	−408.10639	37.3	4.7	85.1	0.6	2.2	0.9
TS1	−408.10533	35.0	4.1	79.2	0.0	−1.3	−0.8
TS2	−408.09903	36.7	4.7	85.0	4.0	5.0	3.8
P1	−408.07830	35.3	4.6	113.1	17.0	17.1	7.5
Formamide	−169.91092	28.5	2.4	61.4			
NaOH	−238.13789	7.2	2.2	55.3			
H_2O	−76.43412	13.3	1.8	45.1			
R2	−792.47538	29.0	4.1	116.3	27.5	26.4	16.4
M4	−792.51914	30.5	4.3	83.0	0.0	0.0	0.0
M5	−792.46955	27.5	4.2	85.1	31.7	28.0	27.3
TS4	−792.45495	27.0	4.4	88.1	40.3	36.9	35.3
P2	−792.44745	26.2	4.3	112.6	45.0	41.3	32.4
NaCl	−622.56446	0.5	1.7	54.9			
HCl	−460.80327	4.2	1.5	44.6			

region. In the first one, collisional heating (activation) of sampled solvated clusters of the protonated peptide drives away the volatile and weakly bound solvent molecules, and brings the protonated peptide and alkali-containing species that are present in the solvated clusters together; as shown in the earlier study [5] and also here, several peptide functional groups may then react with the alkali hydroxide or chloride to form the $[M - nH + mX]^{(m-n)+}$ ions. In the second scenario, naked protonated peptides may collide with alkali hydroxide or chloride molecules that are sampled into the lens region [5], which begins at a near atmospheric pressure at the orifice and ends at a pressure of a few mtorr at the exit of the quadrupolar lens. The relatively high pressure in the lens region ensures a very large number of collisions. A simulation of the motion of an ion, having an initial kinetic energy of 10 eV, an m/z ratio of 190, and a collision cross section of 125 Å^2, through a quadrupolar lens at a pressure of 4 mtorr and an axial potential gradient of 5 V/m, gives an average number of collisions of 100 [22]. Irrespective of the molecular process or reaction sequence, peptide ions are brought into close proximity of alkali-containing species and under conditions of collisional activation. Calculations performed on models of peptide functional groups reacting with alkali hydroxide, chloride, and hydrate show that many of these reactions are feasible as they are either exothermic or endothermic by less than 20 kcal/mol, an amount accessible via collisional activation, and they proceed with no significant barriers. Considering the electrospray sampling conditions, it is likely that both processes are at work.

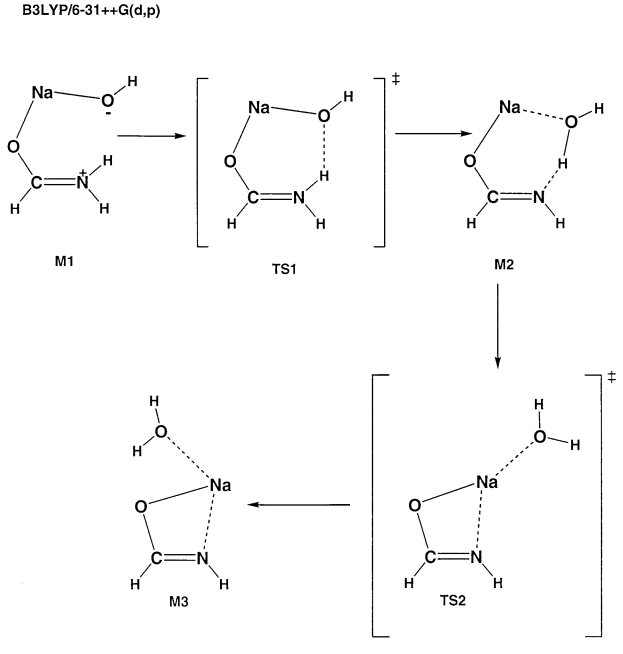

Scheme 1.

Concluding Remarks

The model reactions discussed in this report are those between neutral functional groups and alkali hydroxide, alkali chloride, and alkali hydrate. The mechanisms depicted in Scheme **1** and Figure 3 are those appropriate for a peptide ion in which the charge site is remote from the reacting functional groups and does not participate in the substitution reaction. We are currently developing a model in which the protonated site catalyzes the substitution reaction. Preliminary work indicates that the reaction between a model protonated dipeptide and sodium chloride to generate the protonated sodium

amide product and hydrogen chloride is exergonic by approximately 12 kcal/mol with a well depth of 24 kcal/mol. Furthermore, the protonation site is regenerated at the end and can catalyze another substitution reaction step. This type of reaction is induced by the charge in contrast to the charge-remote mechanism proposed in this study. The reactions between electrosprayed peptide ions and alkali species may take place via both charge-remote and charge-proximal routes, depending on the positioning of the alkali species when they contact the peptide ion.

A reviewer of this paper suggested experiments should be carried out with the model compounds, N-methylacetamide, acetic acid, and 1-propanamide. Electrospraying these compounds in the presence of sodium ions produces sodiated products. These adducts could be interpreted as products of simple adduction of Na^+ to the ligand or as protonated products of substitution reactions, i.e., protonated sodium N-methylacetamide, acetate, and 1-propanamide. Electrospraying compounds containing monofunctional groups will not produce ions in which unambiguous substitution of a proton by an alkali metal ion has occurred. A second question was also raised as to the effect of the protein's three-dimensional structure on the extent of alkali-metal ion incorporation. This effect is unknown; it is possible that a more compact structure in which most of the functional groups are buried may exhibit less alkali-metal ion incorporation than a more extended structure. To know this is, however, beyond the means and intentions of this current investigation.

Acknowledgments

Technical assistance from Steve Quan is gratefully acknowledged. This study was supported by grants from the Natural Science and Engineering Research Council of Canada (NSERC), MDS SCIEX, Canadian Foundation for Innovation (CFI), Ontario Innovation Trust (OIT), and York University.

References

1. Fenn, J. B.; Mann, M.; Meng, C. K.; Wong, S. F.; Whitehouse, C. M. *Science* **1989,** *246*, 64–70.
2. Kebarle, P.; Ho, Y. In *Electrospray Ionization Mass Spectrometry*; Cole, R. B., Ed.; Wiley: New York, 1997; pp 3–63.
3. Smith, R. D.; Loo, J. A.; Ogorzalek Loo, R. R.; Busman, M.; Udseth, H. R. *Mass Spectrom. Rev.* **1991,** *10*, 359–451.
4. Neubauer, G.; Anderegg, R. J. *Anal. Chem.* **1994,** *66*, 1056–1061.
5. Rodriquez, C. F.; Fournier, R.; Chu, I. K.; Hopkinson, A. C.; Siu, K. W. M. *Int. J. Mass Spectrom.* **1999,** *192*, 303–317.
6. Sigel, H.; Martin, R. B. *Chem. Rev.* **1982,** *82*, 385–426.
7. Becke, A. D. *J. Chem. Phys.* **1993,** *98*, 5648–5652.
8. (a) Lee, C.; Yang, W.; Parr, R. G. *Phys. Rev. B* **1988,** *37*, 785–789; (b) Miehlich, B.; Savin, A.; Stoll, H.; Preuss, H. *Chem. Phys. Lett.* **1989,** *157*, 200–206.
9. (a) Krishnan, R.; Binkley, J. S.; Seeger, R.; Pople, J. *J. Chem. Phys.* **1980,** *72*, 650–654; (b) McLean, A. D.; Chandler, G. S. *J. Chem. Phys.* **1980,** *72*, 5639–5648; (c) Chandrasekhar, J.; Andrade, J. G.; Schleyer, P. v. R. *J. Am. Chem. Soc.* **1981,** *103*, 5609–5612. (d) Chandrasekhar, J.; Spitznagel, G. W.; Schleyer, P. v. R. *J. Comput. Chem.* **1983,** *4*, 294–301. (e) Curtiss, L. A.; McGrath, M. P.; Blaudeau, J. P.; Davis, N. E.; Binning, R. C., Jr.; Radom, L. *J. Chem. Phys.* **1995,** *103*, 6104–6113.
10. Gaussian 98, Revision A.5: Frisch, M. J.; Trucks, G. W.; Schlegel, H. B.; Scuseria, G. E.; Robb, M. A.; Cheeseman, J. R.; Zakrzewski, V. G.; Montgomery, J. A.; Stratmann, R. E., Jr.; Burant, J. C.; Dapprich, S.; Millam, J. M.; Daniels, A. D.; Kudin, K. N.; Strain, M. C.; Farkas, O.; Tomasi, J.; Barone, V.; Cossi, M.; Cammi, R.; Mennucci, B.; Pomelli, C.; Adamo, C.; Clifford, S.; Ochterski, J.; Petersson, G. A.; Ayala, P. Y.; Cui, Q.; Morokuma, K.; Malick, D. K.; Rabuck, A. D.; Raghavachari, K.; Foresman, J. B.; Cioslowski, J.; Ortiz, J. V.; Stefarnov, B. B.; Liu, G.; Liashenko, A.; Piskorz, P.; Komaromi, I.; Gomperts, R.; Martin, R. L.; Fox, D. J.; Keith, T.; Al-Laham, M. A.; Peng, C. Y.; Nanayakkara, A.; Gonzalez, C.; Challacombe, M.; Gill, P. M. W.; Johnson, B.; Chen, W.; Wong, M. W.; Andres, J. L.; Gonzalez, C.; Head-Gordon, M.; Replogle, E. S.; Pople, J. A., Gaussian Inc., Pittsburgh, PA, 1998.
11. Lias, S. G.; Bartmess, J. E.; Liebman, J. F.; Holmes, J. L.; Levin, R. D.; Mallard, W. G. *J. Phys. Chem. Ref. Data* **1988,** *17*, Suppl. 1.
12. Lias, S. G.; Lieman, J. F.; Levin, R. D.; Kafafi, S. A. *NIST Standard Reference Database 25*, Version 2.02, 1994.
13. Bartmess, J. E. *NIST Standard Reference Database 19B*, Version 3.01, 1993.
14. (a) Hunter, E. P.; Lias, S. G. In *NIST Chemistry WebBook*, http://webbook.nist.gov/chemistry/; (b) Hunter, E. P.; Lias, S. G. *J. Phys. Chem. Ref. Data* **1998,** *27*, 413–656.
15. Shoeib, T.; Milburn, R. K.; Koyanagi, G. K.; Lavrov, V. V.; Bohme, D. K.; Siu, K. W. M.; Hopkinson, A. C. *Int. J. Mass Spectrom.* **2000,** *201*, 87–100.
16. Holland, P. M.; Castleman, A. W., Jr. *J. Chem. Phys.* **1982,** *76*, 4195–4205.
17. El Aribi, H.; Shoeib, T.; Ling, Y; H.; Hopkinson, A. C.; Siu, K. W. M. Proceedings of the 48th ASMS Conference on Mass Spectrometry and Allied Topics, Long Beach, California, June 11–15, 2000.
18. Rodgers, M. T.; Armentrout, P. B. *J. Phys. Chem. A* **1997,** *101*, 2614–2625.
19. Iribarne, J. V.; Thomson, B. A. *J. Chem. Phys.* **1976,** *64*, 2287–2294.
20. Zhan, D.; Rosell, J.; Fenn, J. B. *J. Am. Soc. Mass Spectrom.* **1998,** *9*, 1241–1247.
21. Rodriguez-Cruz, S. E.; Klassen, J. S.; Williams, E. R. *J. Am. Soc. Mass Spectrom.* **1999,** *10*, 958–968.
22. Simulation was performed on a proprietary program of MDS SCIEX for modeling transport of ions through quadrupoles.